Inelastic Transport and Low-Bias Rectification in a Single-Molecule Diode

Joshua Hihath,[†,‡] Christopher Bruot,[†] Hisao Nakamura,[§] Yoshihiro Asai,[§,*] Ismael Díez-Pérez,[†,⊥] Youngu Lee,[¶] Luping Yu,[#,*] and Nongjian Tao[†,*]

[†]The Center for Bioelectronics and Biosensors, Biodesign Institute, Arizona State University School of Electrical, Energy and Computer Engineering, 1001 S. McAllister Avenue, Tempe, Arizona 85281-5801, United States, [‡]Department of Electrical and Computer Engineering, University of California, Davis, One Shields Avenue, Davis, California 95616, United States, [§]Nanosystem Research Institute (NRI), "RICS", National Institute of Advanced Industrial Science and Technology (AIST), Central 2, Umezono 1-1-1, Tsukuba, Ibaraki 305-8568, Japan, [⊥]Department of Physical Chemistry, University of Barcelona (UB), Barcelona 08028, Spain, [¶]Energy Systems Engineering, Daegu Gyeongbuk Institute of Science and Technology (DGIST), 50-1, Sang-ri, Hyeonpung-myeon, Dalseong-gun, Daegu, Korea, and [#]Department of Chemistry and The James Frank Institute, The University of Chicago, 929 E 57th Street, Chicago, Illinois 60637, United States

ABSTRACT Designing, controlling, and understanding rectification behavior in molecular-scale devices has been a goal of the molecular electronics community for many years. Here we study the transport behavior of a single molecule diode, and its nonrectifying, symmetric counterpart at low temperatures, and at both low and high biases to help elucidate the electron–phonon interactions and transport mechanisms in the rectifying system. We find that the onset of current rectification occurs at low biases, indicating a significant change in the elastic transport pathway. However, the peaks in the inelastic electron tunneling (IET) spectrum are antisymmetric about zero bias and show no significant changes in energy or intensity in the forward or reverse bias directions, indicating that despite the change in the elastic transmission probability there is little impact on the inelastic pathway. These results agree with first principles calculations performed to evaluate the IETS, which also allow us to identify which modes are active in the single molecule junction.

KEYWORDS: molecular electronics · STM-break junction · inelastic electron tunneling spectroscopy · IETS · single-molecule conductance

The critical dimensions of semiconductor devices have decreased exponentially over the past 5 decades, and production devices now have gate lengths of less than 50 nm. As the physical dimensions of these devices have continued to scale-down, the power density has scaled-up, and heat dissipation is now one of the most critical problems in conventional electronics. Meanwhile the field of molecular electronics has made significant progress in contacting, measuring, and developing novel electronic molecular devices.[1] These advances have yielded a better understanding of charge transport in molecular-scale systems and have led to the demonstration of molecular transistors, diodes, and wires.[2] However, even with these improvements, information about electron–phonon coupling and heat dissipation in single molecule systems with explicit device implications has been difficult to extract.[3] These issues, compounded with the fact that the specific configuration and contact geometry within a single molecule junction are typically unknown, has led to the emergence of inelastic electron tunneling spectroscopy (IETS) as an extremely important method for characterizing molecular-scale devices.[4−12] This technique, an all electronic spectroscopy method, provides a direct chemical signature of *the* molecule within the junction,[13] and can provide information about the contact geometry and molecular configuration,[14,15] the transport pathway,[16] the phonon lifetimes within the junction,[17] and critically, information about electron–phonon coupling and power dissipation within these devices.[18,19] However, to date most IETS studies performed on single molecules bound to two electrodes have focused on simple, small, symmetric molecules.[8−10,20,21] These molecules typically have a small number of vibration modes, and even fewer theoretically predicted IET active modes. In this report, we describe the transport behavior of a single molecule diode, a molecule with explicit device implications, to understand the effects that changes in the elastic transport pathway have on phonon excitation and inelastic transport channels. Phonon excitation is an extremely important issue in conventional electronics, and understanding the effects of inelastic transport on molecular scale devices is of paramount importance for creating future devices. Interestingly, we find that although the molecule exhibits a large rectification ratio in both the low and high bias regimes at 4.2 K, the asymmetry in the inelastic current (and IET spectrum) is much weaker than expected. Although this finding is contrary to the predictions of a single-level transport model assuming symmetric coupling,[18] the results agree well with

* Address correspondence to yo-asai@aist.go.jp, lupingyu@uchicago.edu, nongjian.tao@asu.edu.

Received for review August 10, 2011 and accepted September 20, 2011.

Published online September 20, 2011
10.1021/nn2030644

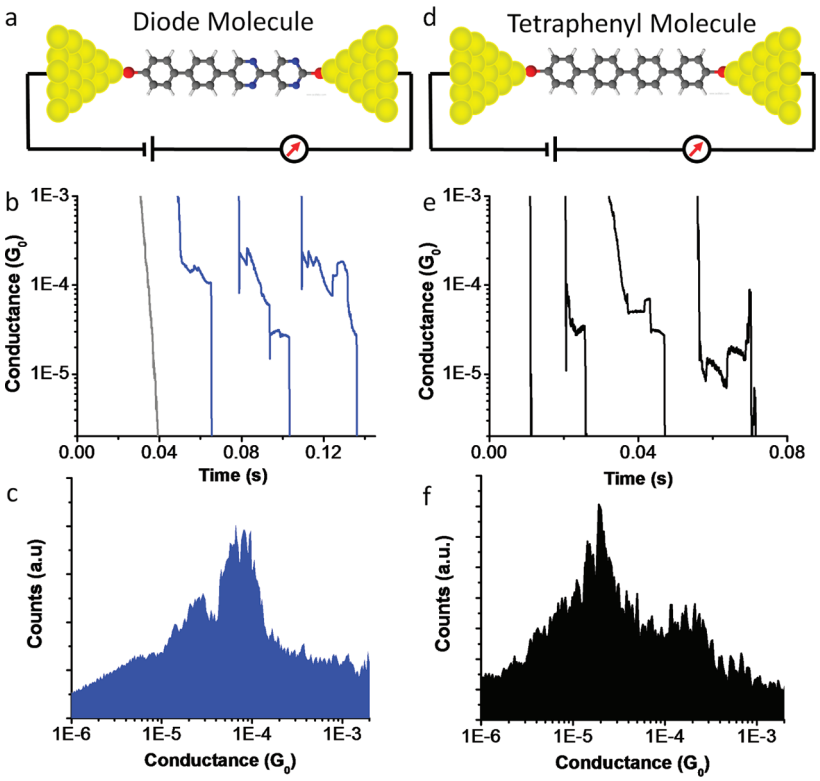

Figure 1. Break junction measurements for the two molecules studied at 4.2 K. (a) Depiction of the diblock molecule that behaves as a molecular diode. (b) Several examples of conductance traces obtained during break junction measurements. Gray curve is an example of when no molecules bind to the two electrodes. (c) Conductance histogram constructed from hundreds of curves similar to those shown in panel b. A clear peak is visible at $\sim 1 \times 10^{-4} G_0$. (d–f) plots equivalent to (a–c), but for the tetraphenyl molecule. The peak in the conductance histogram in panel f is $\sim 2.5 \times 10^{-5} G_0$.

a transport calculation based on non-equillibrium Green's function with density functional theory (NEGF-DFT), indicating that both the inelastic and elastic transport processes are sensitive to bias dependent changes in the electronic coupling.

The field of molecular electronics was originally ignited by the vision of a single molecule rectifier by Aviram and Ratner.[22] In this scheme, a donor group and acceptor group were separated by a sigma-bonded bridge.[23] Although this design proved to be difficult to implement experimentally, in recent years a variety of molecular rectifiers and diodes have been demonstrated using Langmuir–Blodgett films,[24,25] self-assembled monolayers (SAMs),[26–28] and in single molecule devices.[29,30] Alternative mechanisms for rectification have also been used to design architectures for computation.[31] Many of the models proposed for rectification require that charge be delocalized on the rectifying molecular device. However, rectification is also possible in a purely tunneling system if the energy barrier is sufficiently asymmetric.[32] In this study, we use the two molecules shown in Figure 1 panels a and d to explore the effects of molecular asymmetry on the conductance and electron–phonon interactions in single molecule junctions. The first molecule, which we have previously demonstrated to behave as a molecular rectifier at room temperature,[30,33] is a dipyrimidinyl–diphenyl diblock system. The dipyrimidinyl block is electron-deficient, and the diphenyl group is electron rich, resulting in an energy diagram reminiscent of a classic pn junction. This molecule will be referred to as the diode molecule throughout the article. The second molecule consists of a tetraphenyl block terminated with two thiols. This symmetric molecule, which differs only in the substitution of the four nitrogen atoms in the diblock molecule with carbon atoms, is used as a control system to explore the differences that can occur in the current inelastic transport when the molecule is symmetric.

RESULTS AND DISCUSSION

To perform IETS on the molecules of interest, it is first necessary to demonstrate that the charge transport is dominated by tunneling. Thus, to begin characterizing the molecular systems we used a break junction approach[34] to compare the low-temperature (4.2 K) conductance values of the molecular junctions to the room temperature values obtained previously.[30] The break junction approach has been described in detail elsewhere,[35,36] but briefly, these measurements are performed by creating a self-assembled monolayer of the target molecules on a gold substrate. Then, an atomically sharp gold wire is brought into contact with the substrate and withdrawn. A bias is applied

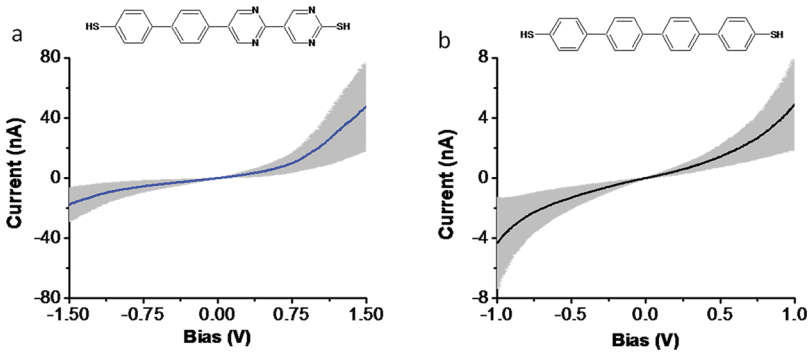

Figure 2. High-bias *I*−*V* characteristics for two molecules. (a) *I*−*V* characteristic for diode molecule with large current asymmetry as a function of bias. (b) *I*−*V* characteristic for tetraphenyl molecule; the trace is symmetric about the zero bias.

between the wire and the substrate and the current between the two is measured as the wire is withdrawn from the surface. When no molecules bind between the tip and the surface a clean exponential decay is observed as is shown in Figure 1b,e (gray curves). However, when a molecule is bound between the two electrodes, clear steps are observed in the current *versus* distance trace, and as the separation continues the current will eventually drop to zero, as is shown in Figure 1b,e (blue and black curves). By performing a statistical analysis of hundreds of these curves it is possible to construct a histogram as is shown in Figure 1c,f, and to determine the most likely conductance of a single molecule junction. The conductance values obtained at 4 K and at 50 mV bias are $\sim 1 \times 10^{-4} G_0$ for the diblock molecule, and $\sim 2.5 \times 10^{-5} G_0$ for the tetraphenyl molecule, where $G_0 = 2e^2/h$. The histograms are constructed from 981 curves for the diode molecule and 165 curves for the tetraphenyl molecule. These conductance values are similar to what was previously obtained at room temperature (see Supporting Information).[30] The temperature independence of the conductance indicates that the conductance is not thermally activated, and that tunneling is likely the dominant transport mechanism.

To determine if changes in the inelastic transport channels depend on changes in the elastic transport, it is necessary to demonstrate that the elastic transport channel changes within the energy range of phonons. Therefore, once the break-junction conductance measurements were performed, it was necessary to characterize the rectification behavior of the two molecules. Although it is in principle possible to measure an *I*−*V* curve of the molecule in question by obtaining conductance histograms at different biases, even though the diode molecule is oriented with the dipyrimidinyl groups away from the substrate during the self-assembly process,[30] during the break junction process the molecules can be reconfigured so that either end is on the substrate electrode, thus adding additional uncertainty to the measurement. Therefore, point-by-point conductance measurements are not preferred for determining the rectification properties of a molecular junction. As such, we used a modified technique to obtain *I*−*V* curves, which we call "pull-and-hold", as is described elsewhere.[8,20,36,37] In this technique the software is modified so that if a step occurs in the current *versus* distance trace while withdrawing the tip from the substrate, the separation process is automatically stopped and the molecule is held in place. This allows the *I*−*V* curves to be obtained from a single molecule where the junction is held in the same configuration throughout the sweep. Although there are cases where the junction breaks down even after the movement is stopped, it is possible to create a large number of junctions for statistical analysis. Figure 2a shows an average of 43 out of a total of 85 *I*−*V* curves obtained from different junctions by sweeping the bias over a ±1.5 V range using the pull-and-hold method to create the molecular junction. In these wide range sweeps, about 35% of the curves obtained displayed significant switching behavior, and were excluded from the average. An additional 15% had rectification in the opposite direction, likely due to a molecule oriented in the opposite direction, the remainder are included in the average. The rectification ratio at 1.5 V is 2.97 ± 1.2, which is similar to the value obtained at room temperature. The gray background shows the standard deviation, and Figure 2b shows an average of 38 *I*−*V* sweeps from the tetraphenyl molecule, showing a clearly symmetric curve in this case. These experiments demonstrate that the rectification behavior is also temperature independent; however, in order to understand any differences in the inelastic current it is also necessary to determine if there is any current asymmetry in the diode molecule at low biases.

After demonstrating that the conductance and high bias *I*−*V* behavior of the two molecules is similar at low temperature to what was previously observed at room temperature, the low-bias behavior of the two systems was characterized in order to determine the conductance asymmetry at low biases, and to explore the effects of molecular and current asymmetry on the electron−phonon coupling in a molecular system. The

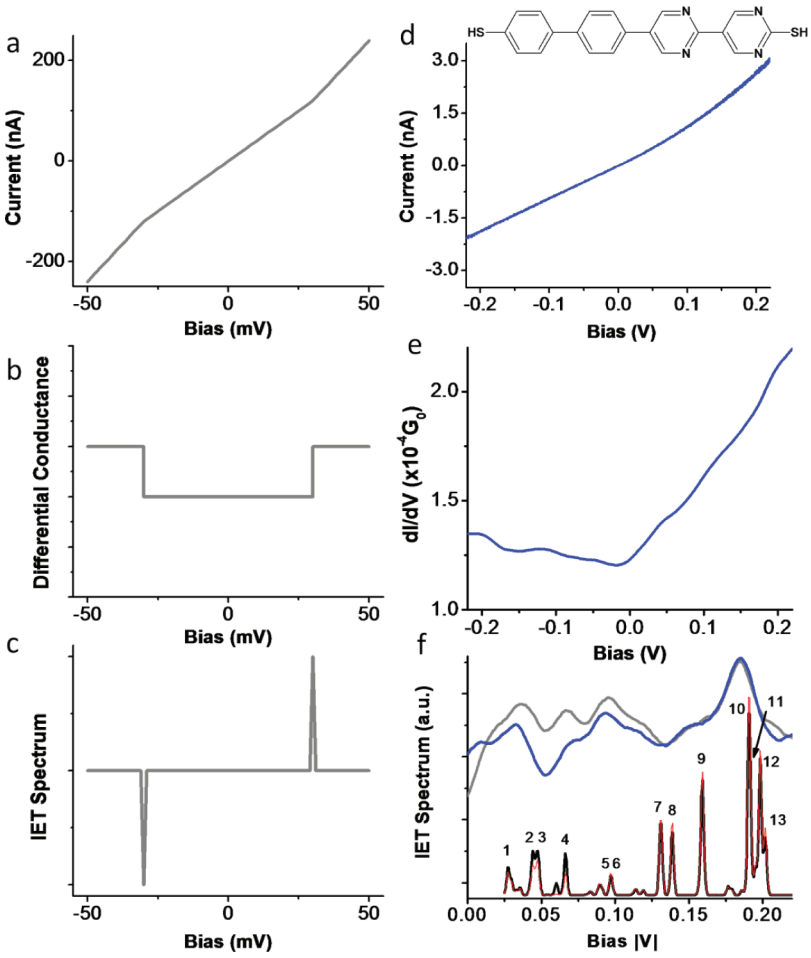

Figure 3. Low bias *I*−*V*, *G*−*V*, and subtracted IET spectra. (a−c) Example of low-bias *I*−*V*, *G*−*V*, and IET measurements. The activation of phonon modes causes a change in the slope of the *I*−*V* curve (a), causes symmetric, step features in the differential conductance (b), and antisymmetric peaks in the IET spectrum (c). (d) Measured *I*−*V* curve for the diode molecule; (e) measured *G*−*V* curve. The *I*−*V* and *G*−*V* curves are clearly asymmetric at low biases, indicating that rectifying behavior is possible even at low biases. (f) Subtracted IET spectra obtained by taking the derivative of panel e and subtracting the slope of the *G*−*V* curve. Blue curve is for positive bias and gray curve is the negative bias region rotated 180°. The phonon features and intensities are similar despite the asymmetry in the conductance. The black and red curves are the calculated IET spectra in forward and reverse bias, respectively.

combined conductance and IET spectroscopy measurements are summarized in Figure 3a−c. In a purely elastic tunneling system, with the molecular energy levels far from the Fermi energy of the electrodes, one would expect the *I*−*V* curve to be linear, and the conductance to be a constant.[38] However, it is also possible to access inelastic tunneling pathways by exciting phonon modes within the molecule.[39,40] In this case, when the bias reaches a threshold voltage $|V_\omega| = \hbar\Omega/e$, it is possible to activate the phonon mode with energy $\hbar\Omega$. This process opens a transport channel in the molecular junction in addition to the primary elastic pathway, and as such causes an increase in the molecule's conductance.[41] This increase in the conductance causes a small change in the slope of the *I*−*V* curve (Figure 3a), but a clear step in the differential conductance (G = d*I*/d*V*), and antisymmetric peaks in the second derivative of the current, d^2I/dV^2. This second derivative curve is referred to as the IET spectrum. It should also be noted that activating a phonon mode depends only on the magnitude of the bias applied, and not on the polarity of the bias. Therefore, the features observed in the *G*−*V* curve are expected to be symmetric with bias, and the IET spectrum is expected to be antisymmetric around zero bias.[37] This means that a phonon mode with an energy of 100 mV will produce a peak at +100 mV and a dip at −100 mV. Thus, to be able to clearly identify the antisymmetric features in the IET spectrum we have plotted $d^2I(V)/dV^2$ and $-d^2I(-V)/dV^2$ on the same plot throughout. This comparison allows us to easily identify antisymmetric features, to compare the peak intensities in the forward and reverse bias directions, and to identify differences in the electron−phonon coupling in the two directions. Identifying antisymmetric features in the IET spectrum is essential for correctly identifying phonon modes, because other types of conductance fluctuations can also yield peaks in the second derivative. However, in these

cases, the features are typically not antisymmetric about zero bias, and as such plotting the spectra in this manner provides clear evidence of phonon activation. Figure 3 panels d–f show averaged *I*–*V*, *G*–*V*, and IET spectra obtained from one junction containing the diode molecule, and Figure 4 panels a–c show these same curves for a tetraphenyl junction.

In addition to information about electron–phonon interactions in a molecular system, the *G*–*V* curve also provides important information about the primary elastic transmission probability. From the *I*–*V* and *G*–*V* curves in Figure 3d,e it is evident that the rectifying behavior in the diblock molecule begins at biases much lower than previously studied.[30] In Figure 3b, it is apparent that the conductance is asymmetric even at values as low as 50 mV. Although the current seems to increase more quickly at high biases (see Figure 2), the conductance appears to increase linearly in the forward bias direction at low biases (<200 mV). This conductance behavior at low bias clearly indicates that the rectification behavior is not dependent on charge delocalization on the molecule as in the cases of the original Aviram–Ratner[22] model or in the Ellenbogen–Love[31] model. Other models have also predicted resonant tunneling through asymmetric barriers to demonstrate rectification behavior,[32] but the onset for resonant tunneling in these systems typically requires higher biases to induce the resonant condition. It seems that none of these models match the rectification behavior observed here. As is discussed briefly below, and in detail elsewhere,[42] we attribute this difference in the conductance in the low-bias region to a change in coupling to the highest occupied molecular orbital (HOMO) and HOMO-1 levels of the molecule when the bias polarity is changed. In particular, clear switching of the conducting orbital from HOMO to HOMO-1 was reported above $V = \pm 0.4$ V.[42]

As is apparent from the asymmetric *G*–*V* curve in Figure 3e, there are significant bias-dependent changes to the elastic transmission probability between forward and reverse bias in the diode molecule. As such, one may expect to observe changes in the inelastic pathway as well. Unfortunately, this asymmetric conductance behavior makes it difficult to discern symmetric step features in the *G*–*V* curve as is anticipated in Figure 3b. However, upon taking the derivative of the *G*–*V* curve to obtain the IET spectra, clear antisymmetric features emerge. The gray curve in Figure 3f is the subtracted IET spectra from the negative bias region, rotated by 180° in order to demonstrate the antisymmetric behavior of the phonon modes. It is worth noting that the phonon modes occur at the same energies in the forward and reverse bias direction despite the differences in current and the inherent dipole of the molecule. This point indicates that even though the potential profile is different in the two bias polarities, there is no impact on the bias required to excite the phonon modes, again

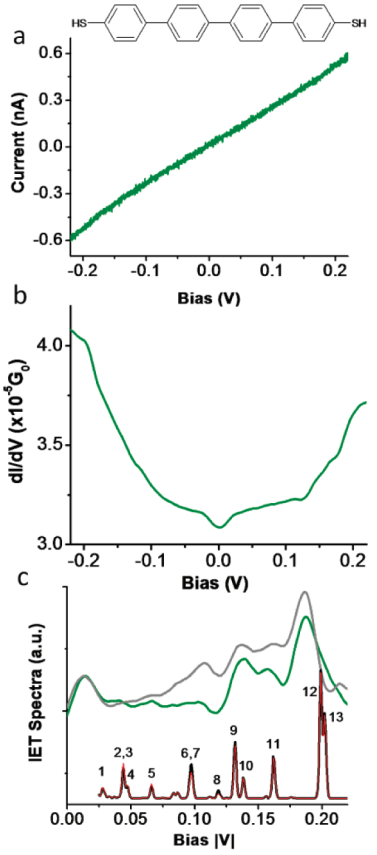

Figure 4. *I*–*V*, *G*–*V*, and IET spectrum for the tetraphenyl molecule. (a) *I*–*V* characteristic for a single junction. (b) Differential conductance obtained with a lock-in amplifier. (c) Experimental IET spectra for the positive bias (green) and negative bias (gray) regions, as well as predicted IET spectrum from first principles calculations for the positive (black) and negative (red) bias regions.

demonstrating that tunneling dominates the transport behavior. Any significant changes in the inelastic transport pathways would be indicated by a change in the intensity of the phonon peaks in the IET spectrum. Therefore, it is necessary to subtract the elastic contributions from the second derivative in order to directly compare peak intensities in the IET spectra. As discussed above, the conductance increase appears to be linear in the low-bias region, so the *G*–*V* curve was fit with a linear function in both the forward and reverse bias directions. Then, the slopes obtained from these fittings were subtracted from the second derivative to yield the subtracted IET spectra in Figure 3f. The spectra obtained using this procedure are referred to as "subtracted IET spectra" in order to avoid confusion with the standard IET spectrum. Although there are some small asymmetries in the intensities of the low-bias modes, the modes at ± 190 mV appear to be nearly identical in both energy and intensity in forward and reverse bias. These small variations in intensity were observed in most of the individual junctions studied, and can even be seen in the spectra from over 100 averaged curves (see Supporting Information). Although these asymmetries in

the peak intensity may be due to either effects from the molecular configuration,[43,44] or from the electronic-vibrational couplings seen in large-scale tunnel junctions,[45−47] they do not show consistent asymmetry across molecular junctions. Furthermore, the asymmetries measured are much smaller than expected from the one-level transport model described below. This observation implies that molecular asymmetry, the inherent molecular dipole, and the magnitude of the current through the device have little impact on the magnitude of the inelastic current within the device. The IET spectrum without any subtraction, as well as the vibration modes associated with each of the number peaks in Figures 3f and 4c are provided in the Supporting Information.

The similarity of phonon intensities in forward and reverse bias indicates that there is no significant change in the inelastic current even when there is a large asymmetry in the elastic current. At first glance, these results seem to be contrary to expectations from the conventional formula based on a single-level model, $\delta I_{\mathrm{inel}} \propto T^2(1-2T) \approx T^2$,[18] where δI_{inel} is the inelastic current and T is transmission probability. Within a single-level/single-site approximation, T at the Fermi level (ε_F) is represented as $T = (\gamma_L\gamma_R)/((\varepsilon_F - \varepsilon_\alpha)^2 + \gamma^2)$. ε_α is an energy level of the bridge molecule, and the terms γ_L and γ_R are related to the imaginary part of the self-energy for the left and right electrodes, respectively. The term γ is an average of γ_L and γ_R, that is, $(\gamma_L + \gamma_R)/2$, which corresponds to the broadening of the energy level due to coupling to the electrodes. Thus, when the above T^2 dependence is assumed, even a modest 10% increase in the transmission probability should yield a ~20% increase in the inelastic current. For the junction in Figure 3, the conductance change between +200 and −200 mV is greater than 50%, indicating that a large change in the IET peak intensity would be expected. However, both experiment and first principles calculations do not yield such a large change in the inelastic current and IET intensity with a change in the bias-polarity.

To determine how large the subtracted IET intensity changes should be in this molecular system, we performed first principles NEGF-DFT calculations including electron−phonon interactions. We adopted the conventional lowest order expansion (LOE) formalism in NEGF-DFT for inelastic transport.[48] We employed the double-ζ plus polarized (DZP) basis for the atoms in the molecule and the anchoring S atoms while using the single-ζ level (SZP) basis for Au atoms. The unit cell was taken as p(4 × 4) with 3 × 3 Monkhorst-Pack k point sampling for both the Green's function and electron−phonon coupling matrices. The frozen phonon approximation was employed, where only atoms of the molecule (including the anchor atoms) were relaxed. The details of the settings for the first principles calculations are given elsewhere.[42] In the present calculation, we omitted low-frequency modes, $\Omega < 150\ \mathrm{cm}^{-1}$, and focused on well-defined molecular internal modes. The results of this calculation (see Figure 3f) agree well with the experimental results, and indicate that any changes in the IET intensity will be small, even if there is a significant change in the transmission probability of the elastic current.

To understand why the inelastic current does not change significantly with a change in the elastic transmission, it is necessary to understand the bias dependence of each of the terms within inelastic current. When the thermal damping of an excited phonon is sufficiently fast, the subtracted IET, which is defined as the second derivative of the inelastic current δI_{inel} by bias V, is expressed as follows:[48]

$$\frac{\mathrm{d}^2(\delta I_{inel})}{\mathrm{d}V^2} = M^2 T \frac{(\varepsilon_F - \varepsilon_\alpha)^2 - \gamma^2}{\{(\varepsilon_F - \varepsilon_\alpha)^2 + \gamma^2\}^2} \frac{\mathrm{d}^2F}{\mathrm{d}V^2}$$

$$= M^2 T \chi \frac{\mathrm{d}^2F}{\mathrm{d}V^2}$$

$$\chi = \frac{(\varepsilon_F - \varepsilon_\alpha)^2 - \gamma^2}{\{(\varepsilon_F - \varepsilon_\alpha)^2 + \gamma^2\}^2} \qquad (1)$$

where M is electron−phonon coupling and F is a function of bias V and phonon frequency Ω. The term $\mathrm{d}^2F/\mathrm{d}V^2$ is an antisymmetric function of V and independent of the electronic structure. Equation 1 omits the energy-dependence of the Green's function and sets it to the value at the Fermi level, ε_F. We note that if γ_L is equal to γ_R, eq 1 leads immediately to the $T^2(1-2T)$ relation as given above.[18] Now, we will consider the ratio: $|(\mathrm{d}^2(\delta I_{\mathrm{inel}})/\mathrm{d}V^2)V|/|(\mathrm{d}^2(\delta I_{\mathrm{inel}})/\mathrm{d}V^2)(-V)|$ based on eq 1 to understand the magnitude of the rectification for elastic and inelastic current. Since the second derivative of the function F is antisymmetric for V and $T(V)/T(-V)$ is larger than 1, the remaining two terms, the ratio of electron−phonon coupling $M(V)/M(-V)$ and $\chi(V)/\chi(-V)$ should be considered.

To estimate the above values, we have to *redefine* the parameters M, ε_α, γ_L, and γ_R from the fully first principle (multilevel and self-consistent) NEGF-DFT result. Use of the effective molecular projected state hamiltonian (MPSH) is a convenient way to analyze first principles results because one can define only the necessary energy levels.[42,49] The terms M, ε_α, γ_L, and γ_R were calculated in the projected molecular orbital (PMO) basis. Thus, we focus on the conducting orbital, φ_α, which dominates the transmission probability, because it is the most important orbital for transport. The details of the effective MPSH method and the physical meanings are given in the Supporting Information. Here, we note only a few important points about the present single-level model and its parameters. First, the coupling terms $\gamma_{L/R}$ are *effective* couplings between the conducting MO on the bridge molecule and any electronic states in the electrodes such as the Bloch and evanescent states, and they include all of the *long-range* transfer integrals. The energy level, ε_α, also consists of the exact energy-shift due to the couplings. Hence, the constructed parameters reflect *any*

nonequilibrium response of the intrinsic electronic structure of the entire junction within the DFT model. As a result, it is natural that these terms depend on the bias (and its polarity) for the diode molecule even though the conformation of anchor atoms and electrodes are symmetric for the left and right sides. The asymmetry due to the bias polarity for γ_L and γ_R comes from an intrinsic property of the present diblock diode molecule and the adopted model is distinct from a simple single level (nearest neighboring) tight-binding model.

In the very low-bias region (<0.3 V), where resonance with phonon modes occurs, a change of bias polarity does not necessarily change whether the conducting MO, φ_α, belongs to the HOMO or HOMO-1 level. However, φ_α spans a sufficiently large range of the electron−phonon coupling to apply conducting MO analysis to both the elastic and inelastic current. For most of the IET active modes, $M(V)/M(-V)$ was lower than 1 below 0.3 V (typically 0.9 at $V = 0.2$ V), although a few modes were slightly larger than 1. The bias polarity dependence of the conducting MO causes a bias-dependence of the effective electron−phonon coupling. In the same bias region, we found that $\chi(V)/\chi(-V)$ is always lower than 1 (*e.g.*, $\chi(0.3)/\chi(-0.3) \approx 0.95$). This is because of the asymmetry of the effective coupling between the conducting MO and the electronic states in the electrodes (*i.e.*, $\gamma^2 > \gamma_L\gamma_R$), as well as the large bias-polarity dependence of the coupling ($\gamma_L(V)\gamma_R(V) \neq \gamma_L(-V)\gamma_R(-V)$) for the present diode molecule. As a result, these intrinsic (bias-induced) electronic structure changes in the diblock diode molecule weaken the expected asymmetry of the inelastic current. We note that in future works additional corrections such as the explicit inclusion of the energy-dependence of the Green's functions, the effects of other PMOs, and the long-tail of the electron−phonon coupling outside of the molecule could be considered to provide a more detailed comparison of the present experimental and theoretical results.

Additionally, to compare the diode molecule's conductance and inelastic transport behavior with a symmetric molecule case we have also included $I-V$, $G-V$, and IET spectra for the tetraphenyl molecule in Figure 4. Clearly, in this junction the $G-V$ curve shows symmetric, step-like features where the phonon modes are activated. There is still some apparent asymmetry in the $G-V$ curve for this junction; however, the ratio of the high conductance value to the low conductance value at 200 mV (1.09) is much smaller than in the diode case (1.57), and the symmetric phonon features are readily apparent in this curve. Additionally, it is common to see some asymmetry in the $G-V$ curves of symmetric molecules because each junction has a unique background due to the specifics of the configuration, contact, and conductance fluctuations due to impurity scattering in the contacts and interference effects.[20,38] Despite these effects it is evident that the IET spectra in the forward (green curve Figure 4c) and reverse (gray curve Figure 4c) bias directions are almost identical. Furthermore, when averaged over a large number of molecular junctions, the $G-V$ curve in the case of the tetraphenyl molecule is symmetric, and in the case of the diode molecule is still asymmetric due to the inherent current asymmetry in the molecular junction, demonstrating that the asymmetry in the low-bias $I-V$ curve is inherent to the diode molecule. These averaged curves are shown in the Supporting Information.

CONCLUSIONS

In summary, we have explored both the high and low-bias conductance behavior of a single molecule diode at cryogenic temperatures. We have shown that the conductance displays clear asymmetry even at biases below 200 mV, that the onset for rectification begins near zero bias, that the transport mechanism is dominated by tunneling, and that despite the asymmetry in the $I-V$ and $G-V$ characteristics at low biases, the IET spectra is antisymmetric with similar phonon energies and intensities in the forward and reverse bias directions. Although contrary to expectations, this result matches well with first principles calculations, and is due to bias-dependent changes in the coupling between the conducting molecular orbital and the electrodes. This finding demonstrates that bias-dependent asymmetry in the electronic coupling is important for both elastic and inelastic processes in the present diblock diode molecule, and that bias dependent changes in the electronic structure should be taken into account for asymmetric systems. Furthermore, the IET spectra agree qualitatively with spectra predicted from first-principles calculations.

EXPERIMENTAL DETAILS

Sample Preparation. The diode molecule and the symmetric tetraphenyl molecule were synthesized according to a reported procedure.[33] SAMs were prepared on a gold substrate then transferred to a cryostat for measurements. In the tetraphenyl case, deprotection of the two symmetric trimethylsilylethyl groups was carried out in a single step using tetrabutylammonium fluoride as the cleaving reagent in an argon purged, distilled tetrahydrofuran (THF) solution that contained 50 mM of the target molecule and an immersed gold substrate prepared using the procedure described below and left overnight. After assembly, the substrate was rinsed successively with THF, hexane, and isopropyl alcohol and dried with nitrogen after each rinsing step.

The SAM of the diode molecule was prepared in two steps. The first step deprotected the cyanoethyl group using sodium ethoxide as the cleaving reagent in argon-purged, distilled THF. Then, a gold substrate was immediately immersed in the solution and left overnight. After the formation of the SAM,

the gold substrate was rinsed thoroughly with THF and then with isopropyl alcohol. For the second deprotection step, the sample was transferred into an argon-purged THF solution to remove the protecting group using the same procedure as described above for the tetraphenyl molecule. This second deprotection reaction lasted over 7 h, after which the gold substrate was rinsed with hexane and ethanol several times and the residual solvent removed by blowing with nitrogen.

The gold substrates were prepared by the thermal evaporation of 130 nm of gold (99.9999% purity, Alfa Aesar) on a freshly cleaved mica surface (Ted Pella, Inc.). The substrates were annealed in a hydrogen flame for approximately 1 min prior to SAM formation. After SAM formation and after being rinsed and dried, the substrate was placed in the homemade STM head along with a newly cut gold tip (99.998% purity Alfa Aesar). The system was then placed in a helium Dewar cryostat (Janis Research Company). The STM chamber was place under a vacuum of 2×10^{-6} Torr before any cryogens were introduced to the system. Once the system stabilized in temperature to ~4.2 K, break junction and IETS measurements were performed. Room temperature measurements were performed in vacuum prior to cooling the STM.

Break Junction and IETS Measurements. Break junction measurements were performed as described in detail previously,[36] and briefly above. The histograms are constructed by plotting each conductance *versus* distance trace in log scale and binning into 400 equally spaced compartments on the conductance axis and adding the resulting single curve histogram to the composite histogram.

IETS measurements were performed in a similar method as the break junction measurements, except that the program was set to stop automatically if a plateau occurred in the current *versus* distance trace. Once the tip withdraw was stopped, the bias between the two electrodes was swept, the current measured with a standard current amplifier, and a lock-in amplifier was used to measure the differential conductance, as has been described in detail previously.[36,50] The IET spectra were obtained by taking the numerical derivative of the $G-V$ curves and smoothing the data using a Savitzky–Golay filter.

Acknowledgment. The authors would like to acknowledge support from the National Science Foundation ECCS-0925498 (J.H. and N.T.), DMR-1004195 (L.P.Y.), and the NSF MRSEC at the University of Chicago (L.P.Y.), as well as the Scientific Research on Innovative Areas, a MEXT Grant-in-Aid Project: "Materials Design through Computics" (No. 23104514) (H.N. and Y.A.), and the Famon y Cajal program and the MC-OIF within the 7th European Commuity framework programme (I.D.P.). J.H. would also like to thank Magnus Paulsson for insightful discussions.

Supporting Information Available: Room temperature conductance histograms for both molecules, an example IET spectrum without subtraction for the diode molecule, averaged IET and $G-V$ curves for both molecules, a table of mode assignments, and a brief description of the theoretical model. This material is available free of charge *via* the Internet at http://pubs.acs.org.

REFERENCES AND NOTES

1. Song, H.; Reed, M. A.; Lee, T. Single Molecule Electronic Devices. *Adv. Mater.* **2011**, *23*, 1583–1608.
2. Tao, N. J. Electron Transport in Molecular Junctions. *Nat. Nanotechnol.* **2006**, *1*, 173–181.
3. Reed, M. A. Inelastic Electron Tunneling Spectroscopy. *Mater. Today* **2008**, *11*, 46–50.
4. Stipe, B. C.; Rezaei, M. A.; Ho, W. Single-Molecule Vibrational Spectroscopy and Microscopy. *Science* **1998**, *280*, 1732–1735.
5. Wang, W.; Lee, T.; Kretzschmar, I.; Reed, M. A. Inelastic Electron Tunneling Spectroscopy of an Alkanedithiol Self-Assembled Monolayer. *Nano Lett.* **2004**, *4*, 643–646.
6. Kushmerick, J. G.; Lazorcik, J.; Patterson, C. H.; Shashidhar, R.; Seferos, D. S.; Bazan, G. C. Vibronic Contributions to Charge Transport across Molecular Junctions. *Nano Lett.* **2004**, *4*, 639–642.
7. Taniguchi, M.; Tsutsui, M.; Yokota, K.; Kawai, T. Inelastic Electron Tunneling Spectroscopy of Single-Molecule Junctions Using a Mechanically Controllable Break Junction. *Nanotechnology* **2009**, *20*, 434008.
8. Hihath, J.; Arroyo, C. R.; Rubio-Bollinger, G.; Tao, N.; Agrait, N. Study of Electron-Phonon Interactions in a Single Molecule Covalently Connected to Two Electrodes. *Nano Lett.* **2008**, *8*, 1673–1678.
9. Okabayashi, N.; Komeda, T. Inelastic Electron Tunneling Spectroscopy with a Dilution Refrigerator Based Scanning Tunneling Microscope. *Meas. Sci. Technol.* **2009**, *20*, 095602.
10. Djukic, D.; Thygesen, K. S.; Untiedt, C.; Smit, R. H. M.; Jacobsen, K. W.; van Ruitenbeek, J. M. Stretching Dependence of the Vibration Modes of a Single-Molecule Pt–H_2–Pt Bridge. *Phys. Rev. B: Condens. Matter* **2005**, *71*, 161402.
11. Song, H.; Kim, Y.; Jang, Y. H.; Jeong, H.; Reed, M. A.; Lee, T. Observation of Molecular Orbital Gating. *Nature* **2009**, *462*, 1039–1043.
12. Cai, L. T.; Cabassi, M. A.; Yoon, H.; Cabarcos, O. M.; McGuiness, C. L.; Flatt, A. K.; Allara, D. L.; Tour, J. M.; Mayer, T. S. Reversible Bistable Switching in Nanoscale Thiol-Substituted Oligoaniline Molecular Junctions. *Nano Lett.* **2005**, *5*, 2365–2372.
13. Hipps, K. W.; Mazur, U. Inelastic Electron Tunneling: An Alternative Molecular Spectroscopy. *J. Phys. Chem.* **1993**, *97*, 7803–7814.
14. Lin, L.-L.; Wang, C.-K.; Luo, Y. Inelastic Electron Tunneling Spectroscopy of Gold-Benzenedithiol-Gold Junctions: Accurate Determination of Molecular Conformation. *ACS Nano* **2011**, *5*, 2257–2263.
15. Solomon, G. C.; Gagliardi, A.; Pecchia, A.; Frauenheim, T.; Di Carlo, A.; Reimers, J. R.; Hush, N. S. Understanding the Inelastic Electron-Tunneling Spectra of Alkanedithiols on Gold. *J. Chem. Phys.* **2006**, *124*, 094704.
16. Troisi, A.; Beebe, J. M.; Picraux, L. B.; van Zee, R. D.; Stewart, D. R.; Ratner, M. A.; Kushmerick, J. G. Tracing Electronic Pathways in Molecules by Using Inelastic Tunneling Spectroscopy. *Proc. Natl. Acad. Sci. U.S.A.* **2007**, *104*, 14255–14259.
17. Paulsson, M.; Frederiksen, T.; Brandbyge, M. Inelastic Transport through Molecules: Comparing First-Principles Calculations to Experiments. *Nano Lett.* **2006**, *6*, 258–262.
18. Paulsson, M.; Frederiksen, T.; Brandbyge, M. Modeling Inelastic Phonon Scattering in Atomic- and Molecular-Wire Junctions. *Phys. Rev. B: Condens. Matter* **2005**, *72*, 201101.
19. Chen, Y.-C.; Zwolak, M.; Di Ventra, M. Inelastic Effects on the Transport Properties of Alkanethiols. *Nano Lett.* **2005**, *5*, 621–624.
20. Arroyo, C. R.; Frederiksen, T.; Rubio-Bollinger, G.; Vélez, M.; Arnau, A.; Sánchez-Portal, D.; Agraït, N. Characterization of Single-Molecule Pentanedithiol Junctions by Inelastic Electron Tunneling Spectroscopy and First-Principles Calculations. *Phys. Rev. B: Condens. Matter* **2010**, *81*, 075405.
21. Taniguchi, M.; Tsutsui, M.; Yokota, K.; Kawai, T. Inelastic Electron Tunneling Spectroscopy of Single-Molecule Junctions Using a Mechanically Controllable Break Junction. *Nanotechnology* **2009**, *20*, 434008.
22. Aviram, A.; Ratner, M. A. Molecular Rectifiers. *Chem. Phys. Lett.* **1974**, *29*, 277–283.
23. Stadler, R.; Geskin, V.; Cornil, J.; Theoretical, A. Study of Substitution Effects in Unimolecular Rectifiers. *Adv. Funct. Mater.* **2008**, *18*, 1119–1130.
24. Martin, A. S.; Sambles, J. R.; Ashwell, G. J. Molecular Rectifier. *Phys. Rev. Lett.* **1993**, *70*, 218–221.
25. Metzger, R. M. Unimolecular Rectifiers: Present Status. *Chem. Phys.* **2006**, *326*, 176–187.
26. Ng, M. K.; Lee, D. C.; Yu, L. P. Molecular Diodes Based on Conjugated Diblock Co-oligomers. *J. Am. Chem. Soc.* **2002**, *124*, 11862–11863.
27. Jiang, P.; Morales, G. M.; You, W.; Yu, L. P. Synthesis of Diode Molecules and Their Sequential Assembly to Control Electron Transport. *Angew. Chem., Int. Ed.* **2004**, *43*, 4471–4475.
28. Chabinyc, M. L.; Chen, X.; Holmlin, R. E.; Jacobs, H.; Skulason, H.; Frisbie, C. D.; Mujica, V.; Ratner, M. A.; Rampi, M. A.; Whitesides, G. M. Molecular Rectification in a Metal–Insulator–Metal Junction Based on Self-Assembled Monolayers. *J. Am. Chem. Soc.* **2002**, *124*, 11730–11736.

29. Elbing, M.; Ochs, R.; Koentopp, M.; Fischer, M.; von Haenisch, C.; Weigend, F.; Evers, F.; Weber, H. B.; Mayor, M.; Single-Molecule Diode., A *Proc. Natl. Acad. Sci. U.S.A.* **2005**, *102*, 8815–8820.
30. Díez-Pérez, I.; Hihath, J.; Lee, Y.; Yu, L. P.; Adamska, L.; Kozhushner, A.; Oleynik, I. I.; N.J., T. Rectification and Stability of a Single Molecular Diode with Controlled Orientation. *Nat. Chem.* **2009**, *1*, 635–641.
31. Ellenbogen, J. C.; Love, J. C. Architectures for Molecular Electronic Computers: 1. Logic Structures and an Adder Designed from Molecular Electronic Diodes. *Proc. IEEE* **2000**, *88*, 386–426.
32. Kornilovitch, P. E.; Bratkovsky, A. M.; Williams, R. S. Current Rectification by Molecules with Asymmetric Tunneling Barriers. *Phys. Rev. B: Condens. Matter* **2002**, *66*, 165436.
33. Morales, G. M.; Jiang, P.; Yuan, S. W.; Lee, Y. G.; Sanchez, A.; You, W.; Yu, L. P. Inversion of the Rectifying Effect in Diblock Molecular Diodes by Protonation. *J. Am. Chem. Soc.* **2005**, *127*, 10456–10457.
34. Xu, B.; Tao, N. J. Measurement of Single-Molecule Resistance by Repeated Formation of Molecular Junctions. *Science* **2003**, *301*, 1221–1223.
35. Hihath, J.; Tao, N. Rapid Measurement of Single-Molecule Conductance. *Nanotechnology* **2008**, *19*, 265204.
36. Hihath, J.; Bruot, C.; Tao, N. J. Electron–Phonon Interactions in Single Octanedithiol Molecular Junctions. *ACS Nano* **2010**, *4*, 3823–3830.
37. Agrait, N.; Untiedt, C.; Rubio-Bollinger, G.; Vieira, S. Onset of Energy Dissipation in Ballistic Atomic Wires. *Phys. Rev. Lett.* **2002**, *88*, 216803.
38. Agrait, N.; Yeyati, A. L.; van Ruitenbeek, J. M. Quantum Properties of Atomic-Sized Conductors. *Phys. Rep.* **2003**, *377*, 81–279.
39. Jaklevic, R. C.; Lambe, J. Molecular Vibration Spectra by Electron Tunneling. *Phys. Rev. Lett.* **1966**, *17*, 1139–1140.
40. Lambe, J.; Jaklevic, R. C. Molecular Vibration Spectra by Inelastic Electron Tunneling. *Phys. Rev.* **1968**, *165*, 821–832.
41. Frederiksen, T.; Paulsson, M.; Brandbyge, M.; Jauho, A. P. Inelastic Transport Theory from First Principles: Methodology and Application to Nanoscale Devices. *Phys. Rev. B: Condens. Matter* **2007**, *75*, 205413.
42. Nakamura, H.; Asai, Y.; Hihath, J.; Bruot, C.; Tao, N. Conducting Orbital Switching by Bias-Induced Electronic Contact Asymmetry in Bipyrimidinyl–Biphenyl Diblock Molecular Diode. *J. Phys. Chem. C* **2011**.
43. Lin, L. L.; Wang, C. K.; Luo, Y. Inelastic Electron Tunneling Spectroscopy of Gold–Benzenedithiol–Gold Junctions: Accurate Determination of Molecular Conformation. *ACS Nano* **2011**, *5*, 2257–2263.
44. Nakamura, H. First-Principles Study for Detection of Inelastic Electron Transport in Molecular Junctions by Internal Substitution. *J. Phys. Chem. C* **2010**, *114*, 12280–12289.
45. Hipps, K. W.; Hoagland, J. J. Top Metal and Bias Effects in the Tunneling Spectrum of Copper(II) Phthalocyanine. *Langmuir* **1991**, *7*, 2180–2187.
46. Mazur, U.; Hipps, K. W. Resonant Tunneling in Metal Phthalocyanines. *J. Phys. Chem.* **1994**, *98*, 8169–8172.
47. Bayman, A.; Hansma, P. K.; Kaska, W. C. Shifts and Dips in Inelastic-Electron-Tunneling Spectra Due to the Tunnel-Junction Environment. *Phys. Rev. B: Condens. Matter* **1981**, *24*, 2449–2455.
48. Nakamura, H.; Yamashita, K.; Rocha, A. R.; Sanvito, S. Efficient *ab Initio* Method for Inelastic Transport in Nanoscale Devices: Analysis of Inelastic Electron Tunneling Spectroscopy. *Phys. Rev. B: Condens. Matter* **2008**, *78*, 235420.
49. Stokbro, K.; Taylor, J.; Brandbyge, M.; Mozos, J. L.; Ordejon, P. Theoretical Study of the Nonlinear Conductance of Di-Thiol Benzene Coupled to Au(111) Surfaces *via* Thiol and Thiolate Bonds. *Comput. Mater. Sci.* **2003**, *27*, 151–160.
50. Petit, C.; Salace, G. Inelastic Electron Tunneling Spectrometer to Characterize Metal-Oxide-Semiconductor Devices with Ultrathin Oxides. *Rev. Sci. Instrum.* **2003**, *74*, 4462–4467.